Increasing Electrical Damping in Energy-Harnessing Transducers

Rajiv Damodaran Prabha, Dongwon Kwon, Orlando Lazaro, Karl D. Peterson, *Graduate Student Members, IEEE*, and Gabriel A. Rincón-Mora, *Fellow, IEEE*

***Abstract*—Wireless microsensors that monitor and detect activity in factories, farms, military camps, vehicles, hospitals, and the human body can save money, energy, and lives [1]. Miniaturized batteries, unfortunately, exhaust easily, which limit deployment to few niche markets. Luckily, harnessing ambient energy offers hope. The challenge is tiny transducers convert only a small fraction of the energy available into the electrical domain, and the microelectronics that transfer and condition power dissipate some of that energy, further reducing the budget on which microsystems rely to operate. Improving transducers and trimming power losses in the system to increase output power is therefore of paramount importance. Increasing the electrical damping force against which transducers work also deserves attention because output power is, fundamentally, the result of damping. This paper explores how investing energy to increase electrical damping can boost output power in electromagnetic, electrostatic, and piezoelectric transducers.**

***Index Terms*—Electrical damping, microsystems, transducers, electromagnetic, electrostatic, piezoelectric, energy harvesters**

I. Powering Microsystems

Harvesting energy from ambient sources (as in Fig. 1) can extend the operational life of a microsystem by recharging a depleting battery. State-of-the-art microscale transducers, however, only generate μW's, of which power-conditioning circuits consume a portion [2]. Fortunately, electrical energy E_E increases with electrical damping force, which as this paper demonstrates, can increase with initially invested energy E_{INV}. To consider this in more detail, Sections II, III, IV and V discuss how investing energy increases output power in electromagnetic, electrostatic, and piezoelectric transducers, drawing relevant conclusions in Section VI.

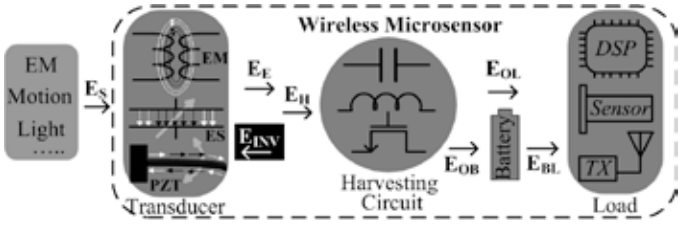

Fig. 1. Sample harvesting wireless microsystem.

II. Electrical Damping

Ambient forces work against and lose energy to damping forces present. An electrical load to the transducer produces one such impeding force (Z_E), but only after losing strength in the domain translation via coupling factor k_C. Source power P_S therefore loses energy in the environment (in Z_S in the model of Fig. 2a) and $k_C^2 Z_E$ to supply output power P_E to Z_E [3]:

$$P_E = \left(\frac{v_S}{Z_S + k_C^2 Z_E}\right)\left(\frac{v_S k_C^2 Z_E}{Z_S + k_C^2 Z_E}\right) = P_S\left(\frac{k_C^2 Z_E}{Z_S + k_C^2 Z_E}\right). \quad (1)$$

As such, substantially low k_C values represent such a light load to the source (i.e., $k_C^2 Z_E << Z_S$) that, while P_S decreases minimally, P_E rises linearly with Z_E, like in Fig. 2b. With higher k_C values, however, $k_C^2 Z_E$ loads P_S to the extent that P_E peaks when $k_C^2 Z_E$ equals Z_S. This means more electrical damping (Z_E) increases P_E, but only if the load to the source ($k_C^2 Z_E$) is less than of all other damping forces present (Z_S).

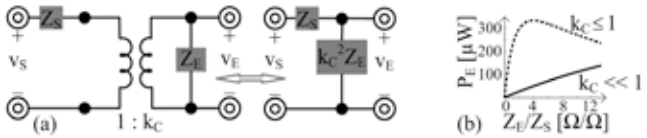

Fig. 2. (a) Equivalent transduction model and (b) resulting output power across electrical damping force Z_E for high and low coupling k_C values.

When k_C is low, as with tiny transducers [4], investing voltage V_{INV} or current I_{INV} energy into the transducer's capacitive (C_H) or inductive (L_H) component raises its electrical damping force. Since a linear rise in voltage Δv_C or current Δi_L demands a linear rise in investment from a battery and the return increases with the square of the voltage in C_H or current in L_H, returns outpace investments. That is, the difference between final and invested energies $E_F - E_{INV}$ (i.e., output energy $E_{H.C}$ in C_H or $E_{H.L}$ in L_H) rises with V_{INV} or I_{INV}:

$$E_{H.C} = E_F - E_{INV} = 0.5C_H(\Delta v_C + V_{INV})^2 - 0.5C_H V_{INV}^2 \quad (2)$$

$$E_{H.L} = E_F - E_{INV} = 0.5L_H(\Delta i_L + I_{INV})^2 - 0.5L_H I_{INV}^2. \quad (3)$$

Here, C_H or L_H harnesses from both Δv_C or Δi_L in $0.5C_H\Delta v_C^2$ or $0.5C_H\Delta i_L^2$ *and* V_{INV} or I_{INV} as $C_H\Delta v_C V_{INV}$ or $L_H\Delta i_L I_{INV}$, which is the gain of investing.

III. Electromagnetic Transducers

An inductor draws electrical energy from a changing magnetic field in the current that it conducts. Accordingly, alternating current in a primary inductor L_P induces variations in its magnetic field, from which a secondary inductor L_S can derive electrical energy. Wireless battery chargers, RF ID, and some biomedical implants harness electromagnetic energy from induced sources this way [5]–[7]. The problem is coupling factor k_C decreases drastically with distance [8], so only

Manuscript received April 30, 2011; revised September 15, 2011. Linear Technology Corporation and Texas Instruments funded this research.

The authors are with the Georgia Tech Analog, Power, and Energy IC Research Laboratory at the School of Electrical and Computer Engineering, Georgia Institute of Technology, Atlanta, GA 30332-0250 U.S.A. (e-mail: rajiv.damodaran@gatech.edu, dkwon3@gatech.edu, orlando.lazaro@ece.gatech.edu, Rincon-Mora@gatech.edu).

applications that can accommodate coupled inductors across short distances thrive today [5]–[6]. Increasing the damping energy can viably extend this distance.

A. Increasing Electrical Damping

Parallel Resonance: L_S in Fig. 3 [7] draws magnetic energy from L_P's alternating field (which secondary EMF voltage $v_{emf.s}$ models) and deposits it into C_S until C_S's voltage v_C surpasses the threshold that the diode-bridge rectifier and battery establish at $2V_D + V_{BAT}$. Because the diodes respond in ns, v_C clamps at $2V_D + V_{BAT}$ and additional energy drawn (in the form of current i_L) flows into V_{BAT} until L_S depletes. As L_P's field (i.e., $v_{emf.s}$) oscillates, C_S first discharges into L_S (so v_C drops to zero) and then L_S charges C_S in the negative direction until v_C clamps to $-2V_D - V_{BAT}$, where additional i_L reaches V_{BAT}. This system, as a result, recycles (i.e., reinvests) C_S's energy back into L_S (rather than into V_{BAT}), increasing L_S's energy and the damping force L_S imposes on L_P's field.

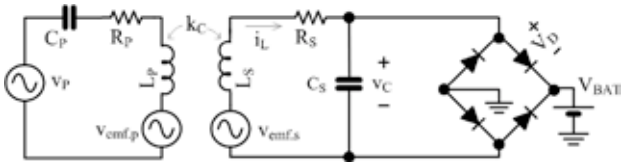

Fig. 3. Coupling electromagnetic energy with a parallel resonant tank.

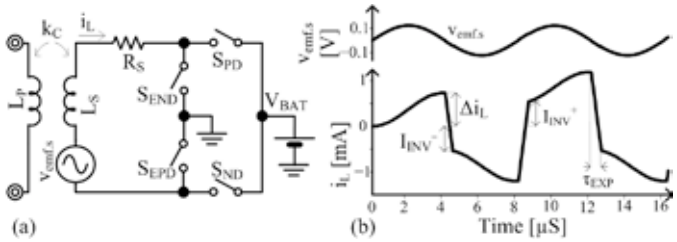

Fig. 4. (a) Proposed capacitor-free converter and (b) simulated waveforms.

Capacitor-free Investment [Proposed]: Assuming k_C is sufficiently low to ensure the loading effect of L_S on L_P's field ($k_C^2 Z_E$ in Fig. 2a) is less than what all other factors represent (Z_S), adding electrical damping energy (Z_E) increases the power the battery receives. Fig. 3 uses C_S's energy for this purpose, but no more than $0.5C_S(2V_D + V_{BAT})^2$ is possible. The proposed circuit of Fig. 4 eliminates this limit by removing C_S and replacing the diodes with synchronous on-chip MOSFETs. Here, S_{EPD} and S_{END} close to allow L_P's field (i.e., $v_{emf.s}$) to energize L_S across positive half-cycle time T_+:

$$\Delta i_L \approx \int_0^{T_+} \frac{V_{EMF.S(PK)} \sin(\omega_O t)}{L_S} dt = \frac{2V_{EMF.S(PK)}}{\omega_O L_S}, \qquad (4)$$

where L_P's field oscillates in response to source EMF voltage $V_{EMF.S(PK)}\sin(\omega_O t)$. Once $v_{emf.s}$'s positive half cycle ends, S_{PD} (and S_{EPD}) close and S_{END} opens to deplete L_S's energy of $0.5L_S\Delta i_L^2$ into V_{BAT}. Keeping S_{EPD} and S_{PD} closed past this point allows i_L to reverse direction (in Fig. 4b), drawing investment energy from V_{BAT} to deposit I_{INV} into L_S.

L_P's alternating field energizes L_S when S_{EPD} and S_{END} again close and S_{ND} and S_{PD} open across $v_{emf.s}$'s negative cycle. i_L continues to increase in the negative direction below I_{INV} by Δi_L because L_S's voltage ($v_{emf.s}$) is still negative, which means L_S's final energy is $0.5L_S(I_{INV} + \Delta i_L)^2$. As a result, S_{END} and S_{ND} de-energize L_S's $0.5L_S\Delta i_L^2$ and $L_S\Delta i_L I_{INV}$ (from Eq. 3) into V_{BAT}, the latter term of which results from investing I_{INV}. The cycle concludes by investing energy in the positive cycle.

B. Performance and Limitations

As stated earlier, increasing electrical damping force is worthwhile as long as it does not load L_P's source field considerably, that is, as long as k_C is low. At 0.06, which is not uncommon [7], Fig. 5 demonstrates that output power P_O increases only when investment remains below 400 μA. At lower k_C values, like at 0.03, more energy is necessary to damp P_S (in Fig. 2a), so P_O peaks at 750 μA. As k_C reduces further, I_{INV} surpasses Δi_L to the extent that conduction losses in the circuit due to I_{INV} dominate. As such, investments beyond a lower threshold do not yield gains. What is more, a higher I_{INV} trades energizing time for investment time, which shifts 0.01's peak further to lower investment values.

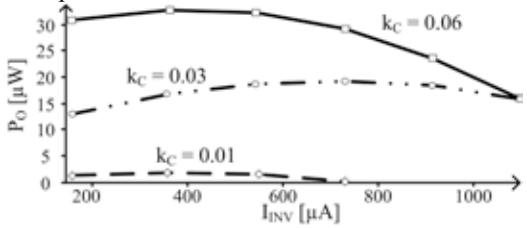

Fig. 5. Simulated P_O across investment values for various coupling factors.

IV. Electrostatic Transducers

A variable capacitor C_{VAR} having one physically suspended plate that moves under the influence of environmental motion can harvest energy. In voltage-constrained (VC) harvesting, because capacitance-voltage product represents charge, maintaining the voltage across C_{VAR} constant when vibrations separate its plates (i.e., decrease capacitance) reduces its charge, which means C_{VAR} produces energy. In charge-constrained (QC) operation, since linear variations in C_{VAR}'s voltage causes squared changes in energy (i.e., E_C is $0.5C_{VAR}v_C^2$), fixing C_{VAR}'s charge by keeping it open when vibrations decrease C_{VAR} raises v_C, so v_C^2 increases surpass linear reductions in C_{VAR} to produce a net energy gain.

A. Increasing Electrical Damping

In both VC and QC operation, the system invests energy at the beginning of each cycle to pre-charge C_{VAR}. Some or all of this charge remains on C_{VAR}'s plates through the harvesting phase to establish an electrostatic attraction that opposes (and damps) the physical movement of the suspended plate. Vibrations, as a result, produce more energy when this electrical damping force (F_{DE}) is higher. In the presence of overpowering mechanical damping forces (when Z_S overwhelms $k_C^2 Z_E$ in Fig. 2), F_{DE} has little impact on the displacement x(t) of C_{VAR}'s plates [4], which means raising F_{DE} draws more electrical energy from vibrations. Therefore, because F_{DE} increases with the square of C_{VAR}'s voltage v_C, as does C_{VAR}'s E_C, higher voltages through the harvesting phase induce more electrical damping in the transducer and, as a result, produce more output energy E_H:

$$E_H = \int F_{DE} dx \propto \int \frac{v_C^2}{x(t)^2} dt \propto \int \frac{E_C}{x(t)^2} dt. \qquad (5)$$

This means that keeping v_C as close to C_{VAR}'s breakdown voltage (V_{MAX}) *throughout* the harvesting period generates more energy than otherwise, which is why VC harvesting at or near V_{MAX} spawns more energy than in QC operation, where v_C rises and nears V_{MAX} only at the end of the cycle [9].

B. Voltage-clamping Capacitor

Constraining C_{VAR}'s voltage with a 2.7 – 4.2-V li-ion battery [10] through the harvesting cycle is one way of extracting energy from motion directly into a battery (V_{BAT}). The advantages of this are that no additional capacitors or energy transfers, which are lossy, are necessary. Unfortunately, V_{BAT} is not the maximum voltage C_{VAR} can sustain, which means C_{VAR} does not draw as much energy as its breakdown voltage allows. So, at the cost of silicon or printed-circuit-board (PCB) area, a large clamping capacitor C_{CLAMP} (of up to 1 nF) that constrains C_{VAR} (e.g., 50 – 250 pF) above V_{BAT} near V_{MAX}, as in Fig. 6, can harness sufficient energy to overcome losses in an additional energy-transfer phase.

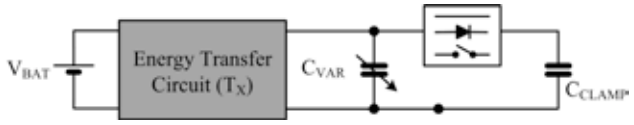

Fig. 6. Constraining C_{VAR}'s voltage with a clamping capacitor.

Permanent Connection: In hard-wiring C_{CLAMP} to C_{VAR} [9], energy-transfer circuit (i.e., T_X) first invests energy E_{INV} from battery V_{BAT} to pre-charge both C_{VAR} and C_{CLAMP} close to V_{MAX}. Then, once the harvesting cycle ends, T_X must fully discharge both capacitors, before C_{VAR} uses remnant energy to help pull its plates together. Because C_{CLAMP} is much higher than C_{VAR} (to ensure C_{CLAMP} clamps C_{VAR} near V_{MAX} when C_{VAR} changes), T_X transfers considerably more energy (E_{INV} and E_H) than it harvests (E_H), so conduction losses are correspondingly higher.

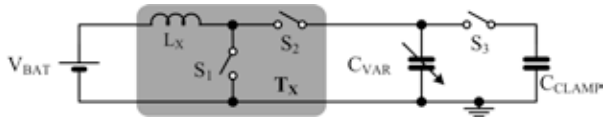

Fig. 7. Proposed electrostatic harvester.

Asynchronous Connection: T_X in [11] pre-charges C_{VAR} to a fraction of V_{MAX} so mechanical energy can raise C_{VAR}'s voltage to a diode voltage above C_{CLAMP}'s initially high voltage (near V_{MAX}) before driving charge into C_{CLAMP}. The interface circuit then transfers harnessed energy in C_{CLAMP} to V_{BAT}. Although T_X transfers less energy because C_{CLAMP} keeps its initial charge, the diode dissipates power and C_{VAR}'s voltage is considerably below V_{MAX} for a substantial portion of the harvesting period.

Managed Connection [Proposed]: Alternatively, T_X in Fig. 7 charges C_{VAR} to C_{CLAMP}'s initial voltage (near V_{MAX}), and once done, the controller closes switch S_3 to steer mechanical energy extracted into C_{CLAMP}. T_X then discharges C_{VAR} into V_{BAT} before vibrations push its plates together, and de-energizes C_{CLAMP} with C_{VAR} (via S_3) less often, when C_{CLAMP} reaches V_{MAX}. As such, C_{VAR} remains close to V_{MAX} through the entire harvesting phase and S_3 dissipates less power than the diode in [11] (because its terminal voltages are considerably lower). Adding intelligence to manage the pre-charge process and the ensuing connection this way, however, requires energy, which represents a loss to the system.

C. Performance and Limitations

The major drawback to C_{CLAMP} is its impact on integration. Unfortunately, reducing capacitance increases C_{CLAMP}'s voltage variation (through the harvesting phase), so its voltage must start further below V_{MAX} (at V_{INI} in Fig. 8) to keep C_{CLAMP} from breaking down. As a result, C_{VAR} harvests less energy per cycle, as E_{OUT} in Fig. 8 shows below 100 pF for a 0.35-µm CMOS circuit with 40-V devices. Interestingly, increasing C_{CLAMP} when permanently connected to C_{VAR} (e.g., above 100 pF in Fig. 8) does not always increase E_{OUT}. This happens because T_X transfers more charge to raise C_{CLAMP} near V_{MAX}, which means additional conduction losses negate the gains of increased electrical damping forces. The circuit proposed in Fig. 7, however, transfers substantially less energy because C_{CLAMP} retains its initial charge through all phases.

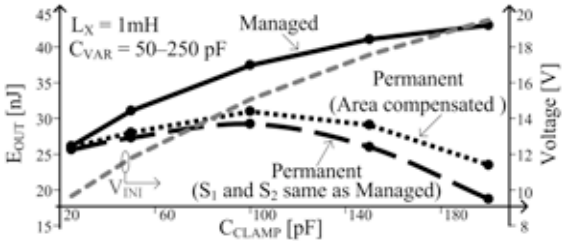

Fig. 8. Simulated output energy across clamping capacitances.

One difference between the two connection strategies is the presence of S_3, which requires silicon area. Removing S_3 and dedicating its area to other switches decreases the resistance across (and conduction losses in) the system, raising E_{OUT}. Reducing resistances by this amount, however, does not compensate for the losses that transferring all of C_{CLAMP}'s charge incurs, as E_{OUT} in Fig. 8 shows. Still, controlling S_3 requires quiescent and switching energy not accounted for in Fig. 8. As a result, managing the connection is better only if conduction losses with a permanent connection exceed controller losses, which is more likely when C_{CLAMP} is higher because higher capacitance requires more energy to charge.

V. Piezoelectric Transducers

A. Battery-coupled Damping

Piezoelectric transducers (PZT) generate charge in response to mechanical vibrations. When open-circuited, the resulting current energizes and de-energizes the capacitance across the surfaces of the device (C_P) and supplies the parasitic leakage across the same (via R_P) [12]. Cascading a full-wave rectifier and a battery V_{BAT} (as in Fig. 9, but without S_{RE} and L_{RE}) steers charge away from C_P into V_{BAT} when PZT current i_P charges C_P above the barrier voltage that conducting diodes and V_{BAT} establish (i.e., $2V_D + V_{BAT}$). V_{BAT} can harness more energy when MOSFETs replace the diodes [13] because the barrier is lower, but only after i_P charges C_P above V_{BAT} [12].

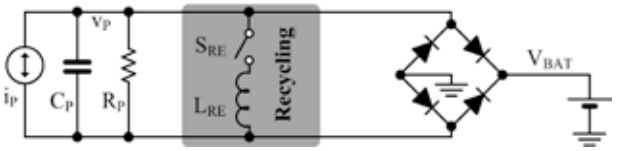

Fig. 9. Recycling inductor L_{RE} into a full-wave rectifier [15].

When unloaded, to be more specific, i_P charges C_P from negative to positive open-circuit voltages $-V_{OC}$ to V_{OC} (by $2V_{OC}$) with charge Q_{OC}, which is $2V_{OC}C_P$. When loaded, the rectifier conducts to V_{BAT} the portion of Q_{OC} that would have charged open-circuited C_P above $|V_{BAT}|$ to $|V_{OC}|$, so V_{BAT} harnesses the difference twice (every half cycle) as

$$E_H = 2(Q_{OC} - 2V_{BAT}C_P)V_{BAT} = 4C_P(V_{OC} - V_{BAT})V_{BAT}, \quad (6)$$

the peak of which happens at $C_PV_{OC}^2$ when V_{BAT} is $0.5V_{OC}$ [14]. Here, vibrations supply and absorb the energy with which they charge and discharge C_P between V_{BAT} and $-V_{BAT}$.

Recycling Inductor: L_{RE} in Fig. 9 [15]–[16] increases E_H by recycling C_P's energy at V_{BAT} to energize C_P in the other direction to $-V_{BAT}$. That is, after the positive half cycle, S_{RE} closes and L_{RE} de-energizes C_P and subsequently (through resonance) supplies the energy L_{RE} stored in the process to charge C_P to $-V_{BAT}$. In this manner, C_P draws no mechanical energy to charge to V_{BAT} and $-V_{BAT}$, so collects all of Q_{OC} as:

$$E_H' = 2Q_{OC}V_{BAT} = 2(2V_{OC}C_P)V_{BAT} = 4C_PV_{OC}V_{BAT}. \quad (7)$$

S_{RE} and the circuit used to control S_{RE} dissipate power, so the energy C_P requires to charge between $-V_{BAT}$ and V_{BAT} every half cycle, which is $2(0.5C_P(2V_{BAT})^2)$ or $4C_PV_{BAT}^2$, should surpass these losses. In the end, drawing energy from vibrations amounts to damping them. With a rectifier, since the transducer ejects Q_{OC} near V_{BAT}, and output energy per half cycle is $Q_{OC}V_{BAT}$, V_{BAT} ultimately limits the electrical damping force from which the transducer harvests energy.

B. Battery-decoupled Damping

One way of further increasing electrical damping force is to decouple V_{BAT} from the transducer. For example, inserting a buck dc–dc converter [16] between the rectifier and V_{BAT} allows Q_{OC} to leave the transducer at a higher voltage (with more energy). The drawbacks to this are higher cost (in components, silicon area, and PCB real estate) and conduction losses (across the switches in the dc-dc converter).

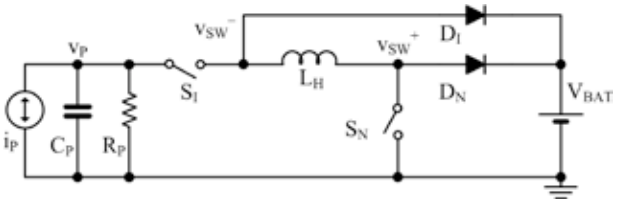

Fig. 10. Rectifier-free piezoelectric harvester [17].

Instead of requiring more lossy components, the buck–boost ac–dc converter–harvester in Fig. 10 [17] decouples V_{BAT} from the transducer by embedding a quasi-lossless inductor (L_H) into its rectifying core. This way, vibrations charge an open-circuited C_P to its maximum possible value before discharging C_P (with S_I and S_N) into L_H (with resonance), and then fully de-energizing L_H into V_{BAT} (with D_N after opening S_N). S_I and S_N similarly discharge C_P into L_H in the negative half cycle and D_I (when S_I opens) de-energizes L_H into V_{BAT}.

Because vibrations energize open-circuited C_P from $-V_{OC}$ to V_{OC} (i.e., $2V_{OC}$) and back, C_P now energizes with $2V_{OC}$ every half cycle and the system fully de-energizes C_P into L_H and then into V_{BAT} every half cycle, which means V_{BAT} receives $0.5C_P(2V_{OC})^2$ twice, or $4C_PV_{OC}^2$ as E_H". This gain is 2× higher than with the best possible recycled rectifier case (highest E_H'), when V_{BAT} is half V_{OC}, and 4× higher than with the best non-recycled rectifier case (highest E_H). The reason for this improvement is that, in charging to a higher voltage ($2V_{OC}$ instead of V_{BAT}), C_P draws more energy from vibrations, which is another way of saying the system imposes more electrical damping force on the transducer.

Reinvesting Energy [Proposed]: Increasing output energy is possible by reinvesting the energy gained in half the cycle (rather than depositing into V_{BAT}) to increase the electrical damping force in the other half. For example, redirecting all the energy C_P draws from vibrations to charge by $2V_{OC}$ to charge C_P in the opposite direction pre-charges C_P to $-2V_{OC}$ so vibrations in the negative half cycle further charge C_P by another $2V_{OC}$ to $-4V_{OC}$. Because the energy in a capacitor increases with the square of its voltage, harnessing what C_P stores at $-4V_{OC}$ once per cycle produces more than drawing C_P's energy twice at half that voltage, at $2V_{OC}$ and $-2V_{OC}$:

$$E_H''' = 0 + 0.5C_P(-4V_{OC})^2 = 8C_PV_{OC}^2. \quad (8)$$

To realize this, after CP_{PK} in Fig. 11 senses that v_P peaks, M_{N1}–M_{N2} and M_{N3}–M_{N4}, which implement S_I and S_N in Fig. 10, close for L_HC_P's half resonance period so that C_P discharges into L_H and L_H subsequently de-energizes back into C_P. Once CP_{PK} senses that open-circuited C_P peaks in the opposite direction, S_I and S_N close to discharge C_P into L_H and S_I alone opens to de-energize L_H into V_{BAT} through M_{PDI}, which together with CP_{DI}, emulates diode D_I.

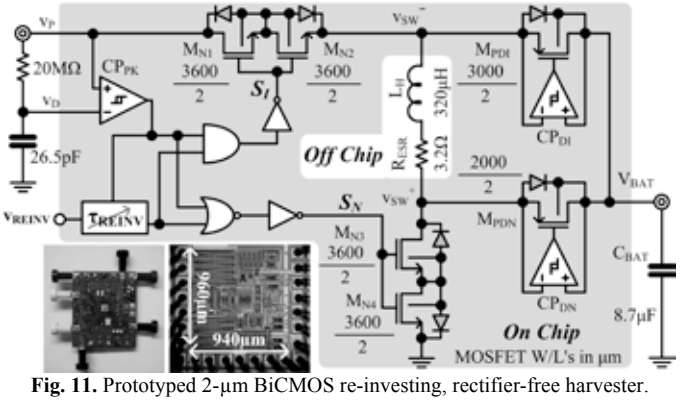

Fig. 11. Prototyped 2-µm BiCMOS re-investing, rectifier-free harvester.

C. Experimental Validation

The prototyped 2-µm BiCMOS harvester tunes the time that S_I and S_N connect (τ_{REINV}) externally with v_{REINV}. Unlike in [17], τ_{REINV} extends beyond L_HC_P's quarter resonance period to a half to reinvest L_H's energy back in C_P. When τ_{REINV} is less than L_HC_P's half resonance period, S_N opens early and L_H drains remnant energy into V_{BAT} via M_{PDN}, which with CP_{DN}, implements D_N. Once tuned, shaking a 44 × 13 × 0.4-mm^3 piezoelectric transducer charged C_P and L_H then recycled C_P's energy at 1.02 V to pre-charge C_P in the opposite direction to –0.36 V, as Fig. 12a shows. Vibrations then charged C_P further

to –1.9 V before L_H de-energized C_P into C_{BAT}. After 2.5 s of repeated cycles, C_{BAT} charged from 2.68 to 4.36 V, as Fig. 12b corroborates. Without reinvesting energy, C_P charged to 1.4 V and –1.2 V to energize C_{BAT} from 2.68 to 4.36 V in 3 s, which under similar conditions, means reinvesting energy produced 20% more output power.

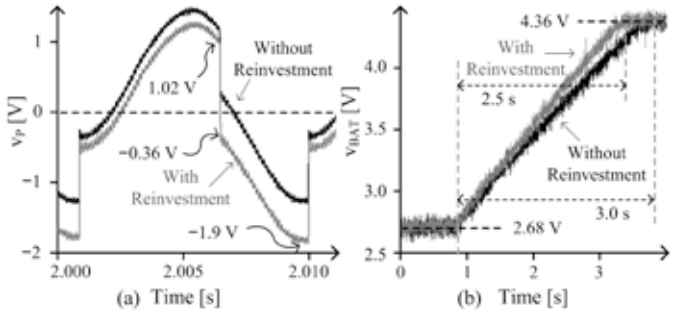

Fig.12. Measured C_P and C_{BAT} charge profiles with and without reinvestment.

D. Performance and Limitations

Notice CP_{PK} is late in detecting v_P's peaks, so before L_H can de-energize C_P, vibrations absorb some of C_P's energy (in both cases shown). Also note that L_H's reinvestment in C_P is unable to charge C_P to –1.02 V because conducting switches (S_N and S_I) and L_H's equivalent series resistance R_{ESR} dissipate some of that energy. This is critical because reducing C_P's negative peak voltage has a squared impact on C_P's peak energy, which is what the system harvests.

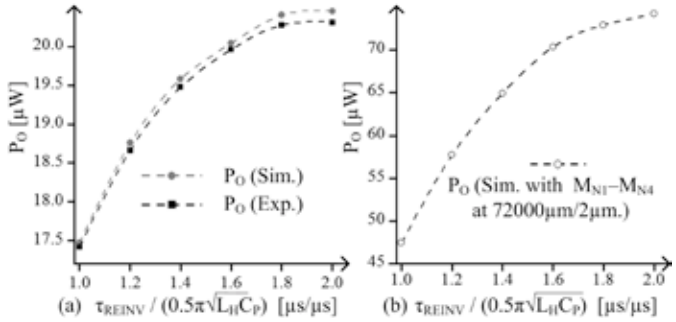

Fig. 13. Experimental and simulated output power across investment time.

Interestingly, as the experimental results of Fig. 13a show, increasing the investment in C_P produces diminishing returns in P_O. This results because transferring more energy through the switches and L_H's R_{ESR} also increases conduction losses to the point they overwhelm reinvestment gains. Enlarging the FETs to lower their resistances [12] balances losses and therefore raises P_O, as the simulated traces of Fig. 13b show. With twenty times (20×) larger FETs for S_N and S_I (at 72000µm/2µm), in fact, fully investing C_P's positive energy into the negative phase raised simulated P_O by 56% from 47.4 µW to 74.2 µW. Ultimately, however, FET losses vary with input power, process, and temperature, but not mismatch.

VI. Conclusions

The experimental results of the piezoelectric transducer and the simulated results of the electromagnetic and electrostatic cases show that *investing* energy into the system *increases* output power P_O. This is important because the coupling factors of tiny transducers and transponding inductors are substantially low, which means P_O is also low. The idea here is to invest energy to raise the electrical damping force against which motion, magnetic fields, etc. work. This way, transducers draw more energy from the environment. The circuit components that transfer the investment, however, consume power, limiting the extent to which increased investments raise P_O. Still, increasing P_O this way, beyond reducing losses in the system, expands the functional reach of miniaturized systems to more practical levels.

References

[1] G. Chen *et al.*, "Circuit Design Advances for Wireless Sensing Applications," *Proc. IEEE*, vol. 98, no. 11, pp. 1808-1827, Nov. 2010.

[2] R.J.M. Vullers *et al.*, "Micropower energy harvesting," *Solid-State Electronics*, vol. 53, no. 7, pp. 684 – 693, Jul. 2009.

[3] S. D. Senturia, "Energy-conserving transducers" in *Microsystem Design*, New York: Springer, 2001, pp. 125-145.

[4] P.D. Mitcheson *et al.*, "Architectures for vibration-driven micropower generators," *J. Microelectromech. Syst.*, vol.13, no. 3, pp. 429- 440, Jun. 2004.

[5] L. Xun and S. Y. Hui, "Simulation study and experimental verification of a universal contactless battery charging platform with localized charging features," *IEEE Trans. Power Electron*, vol. 22, pp. 2202-2210, Nov. 2007.

[6] M. Kiani and M. Ghovanloo, "An RFID-based closed-loop wireless power transmission system for biomedical applications," *IEEE Trans. Circuits Syst. II*, vol. 57, pp. 260-264, Apr. 2010.

[7] M. W. Baker and R. Sarpeshkar, "Feedback analysis and design of RF power links for low-power bionic systems," *IEEE Trans. Biomed. Circuits Syst.*, vol. 1, pp. 28-38, 2007.

[8] C. Chih-Jung *et al.*, "A study of loosely coupled coils for wireless power transfer," *IEEE Trans. Circuits Syst. II*, vol. 57, pp. 536-540, Jul. 2010.

[9] S. Meninger *et al*., "Vibration-to-electric energy conversion," *IEEE Trans. Very Large Scale Integr. (VLSI) Syst.*, vol. 9, pp. 64-76, Feb. 2001.

[10] E. O. Torres and G. A. Rincon-Mora, "A 0.7-µm BiCMOS electrostatic energy-harvesting system IC," *IEEE J. Solid-State Circuits*, vol. 45, pp. 483-496, Feb. 2010.

[11] B. C. Yen and J. H. Lang, "A variable-capacitance vibration-to-electric energy harvester, " *IEEE Trans. Circuits Syst. I*, vol. 53, pp. 288-295, Feb. 2006.

[12] D. Kwon *et al*., "Harvesting ambient kinetic energy with switched-inductor converters," *IEEE Trans. Circuits Syst. I,* vol. 58, no. 7, pp.1551–1560, July 2011.

[13] H. Lam *et al*., "Integrated low-loss CMOS active rectifier for wirelessly powered devices," *IEEE Trans. Circuits Syst. II*, vol. 53, no. 12, pp. 1378–1382, Dec. 2006.

[14] G.K. Ottman *et al*., "Adaptive piezoelectric energy harvesting circuit for wireless remote power supply," *IEEE Trans. Power Electron.*, vol. 17, no. 5, pp. 669–676, Sep. 2002.

[15] E. Lefeuvre *et al.*, "A comparison between several vibration-powered piezoelectric generators for standalone systems," *Sensors and Actuators A*, vol. 126, pp. 405–416, 2006.

[16] Y.K. Ramadass and A.P. Chandrakasan, "An efficient piezoelectric energy harvesting interface circuit using a bias-flip rectifier and shared inductor," *IEEE J. Solid-State Circuits*, vol. 45, no. 1, pp. 189–204, Jan. 2010.

[17] D. Kwon and G.A. Rincón-Mora "A 2-µm BiCMOS rectifier-free AC-DC piezoelectric energy harvester-charger IC," *IEEE Trans. Biomedical Circuits Syst.*, vol. 4, no. 6, pp. 400–409, Dec. 2010.